BMC Plant Biology

RESEARCH

Open Access

Nitrogen starvation leads to TOR kinase-mediated downregulation of fatty acid synthesis in the algae *Chlorella sorokiniana* and *Chlamydomonas reinhardtii*

Jithesh Vijayan[1,2,3*], Sophie Alvarez[4], Michael J. Naldrett[4], Wyatt Morse[1], Amanda Maliva[1], Nishikant Wase[5] and Wayne R. Riekhof[1]

Abstract

Background When subject to stress conditions such as nutrient limitation microalgae accumulate triacylglycerol (TAG). Fatty acid, a substrate for TAG synthesis is derived from *de novo* synthesis or by membrane remodeling. The model industrial alga *Chlorellasorokiniana* accumulates TAG and other storage compounds under nitrogen (N)-limited growth. Molecular mechanisms underlying these processes are still to be elucidated.

Result Previously we used transcriptomics to explore the regulation of TAG synthesis in *C. sorokiniana*. Surprisingly, our analysis showed that the expression of several key genes encoding enzymes involved in plastidic fatty acid synthesis are significantly repressed. Metabolic labeling with radiolabeled acetate showed that *de novo* fatty acid synthesis is indeed downregulated under N-limitation. Likewise, inhibition of the Target of Rapamycin kinase (TOR), a key regulator of metabolism and growth, decreased fatty acid synthesis. We compared the changes in proteins and phosphoprotein abundance using a proteomics and phosphoproteomics approach in *C. sorokiniana* cells under N-limitation or TOR inhibition and found extensive overlap between the N-limited and TOR-inhibited conditions. We also identified changes in the phosphorylation status of TOR complex proteins, TOR-kinase, and RAPTOR, under N-limitation. This indicates that TOR signaling is altered in a nitrogen-dependent manner. We find that TOR-mediated metabolic remodeling of fatty acid synthesis under N-limitation is conserved in the chlorophyte algae *Chlorella sorokiniana* and *Chlamydomonas reinhardtii*.

Conclusion Our results indicate that under N-limitation there is significant metabolic remodeling, including fatty acid synthesis, mediated by TOR signaling. This process is conserved across chlorophyte algae. Using proteomic and phosphoproteomic analysis, we show that N-limitation affects TOR signaling and this in-turn affects the metabolic status of the cells. This study presents a link between N-limitation, TOR signaling and fatty acid synthesis in green-lineage.

Keywords Microalgae, Chlorella sorokiniana, Nitrogen limitation, Fatty acid synthesis, Lipid metabolism, Target of Rapamycin

*Correspondence:
Jithesh Vijayan
jitheshbt@huskers.unl.edu
Full list of author information is available at the end of the article

Background

Algae as a feedstock for biofuels and other bioproducts has been investigated over the last 50 years, owing to the potential for high biomass yield, accumulation of large quantities of neutral lipids, sequestration of carbon dioxide, and capability of growth on marginal lands and in brackish wastewater [1]. Triacylglycerol (TAG) derived from biological sources can be transesterified and blended with crude oil-derived diesel for burning in Diesel engines, and can serve as a feedstock to produce jet fuel and other hydrocarbon-based products [2, 3]. Microalgae accumulate TAG under certain stress conditions, such as nutrient limitation [4] or chemical stressors [5], and the mechanism by which macronutrient limitation induces TAG accumulation has been the subject of many studies for the past five decades [6–8]. Fatty acids for TAG synthesis can be derived either from de novo synthesis or by membrane remodeling, i.e., the process of channeling fatty acids and glycerol from other membrane glycerolipids, such as monogalactosyldiacylglycerol and phosphatidylcholine [8–13].

In the plant lineage, fatty acid synthesis occurs in the chloroplast, and Acetyl CoA Carboxylase (ACCase) and Fatty Acid Synthase complex (FAS) enzymes are similar to the prokaryotic multiple-subunit "type II" synthases [14]. Carboxylation of acetyl-CoA to malonyl-CoA catalyzed by ACCase is the first committed step in fatty acid biosynthesis. FAS complex uses malonyl-CoA to sequentially add 2-carbon units to the nascent fatty acid, ultimately forming a 16–18 carbon chain [15]. Fatty acid synthesis is a major sink of ATP and reducing equivalents and is hence highly regulated [16].

Target of Rapamycin (TOR) is a phosphatidylinositol-3-kinase like serine/threonine kinase that is present in all eukaryotes and is known to regulate metabolism in response to a variety of cues, such as hormones, nutrients, and cellular or organismal energy status. It is known to be a nexus connecting nutrient sensing, growth, and metabolism, acting in the regulatory module of SnRK1/TOR [17]. TOR kinase functions as a complex and in green lineage, there are three known proteins forming the complex: TOR kinase, RAPTOR, LST8 [18]. In yeast and humans, there are two TOR complexes, TORC1 and TORC2. Both complexes have TOR-kinase and LST8 as common members, and the presence of RAPTOR (TORC1) or RICTOR (TORC2) determines the identity and function of the complex [19]. In plants and algae lack RICTOR and hence TORC2 is absent [18]. Role of TOR signaling in photosynthesis [20, 21], amino acid synthesis [21, 22], redox regulation [23, 23], autophagy [24] and TAG accumulation [25] has been established in microalgae.

Chlorella sorokiniana is a microalga belonging to the family Trebouxiophyceae. It is an industrial microalga with high growth potential [26] with the ability to grow on municipal and agricultural wastewater [27]. *C. sorokiniana* genome is sequenced and well characterized and annotated [28]. In this article, we show that fatty acid synthesis is decreased under nitrogen limitation. We further show that this regulation of fatty acid synthesis is, at least partly, controlled by TOR signaling in the microalgae *C. sorokiniana* and *Chlamydomonas reinharditii.*

Results

Nitrogen starvation in *C. sorokiniana* leads to a decrease in the rate of fatty acid biosynthesis

In a previous transcriptomic analysis of *Chlorella sorokiniana* cultures under N-limitation, we observed that many genes encoding key enzymes in various steps of fatty acid synthesis are downregulated as depicted in Fig. S1A-B [12]. Transcript abundances of Ketoacyl-ACP-Synthase 1 (KAS1), 3 (KAS3), Hydroxyacyl-ACP-Dehydratase (HAD1) and Enoyl Reductase (ENR1) are significantly decreased. These enzymes are components of the plastidic FAS complex as outlined in the introduction. The observed downregulation of these genes prompted us to hypothesize that fatty acid synthesis is decreased in N-limited cultures. To test this hypothesis, we carried out metabolic labeling studies with ^{14}C-acetate under N-replete and -limited conditions after 24 h of growth. The experiment was carried out with 10^7 cells for each condition and experimental replicates. Under N-limitation, incorporation of ^{14}C-acetate into fatty acid is significantly decreased, as shown in Fig. 1A and B. We also observed no significant increase in total fatty acid content in cultures under N-limitation, on a per cell basis (Fig. 1C). While there is no significant increase in total fatty acid content, we observed changes in fatty acid compositions, with oleic (18:1) and linoleic acid (18:2) increasing in abundance, and linolenic acid (18:3) and its 16-carbon counterpart ($16:3^{\Delta 7,10,13}$) decreasing in abundance (Fig. 1D). Incorporation of acetate into fatty acid is decreased, but the flux of existing fatty acids into TAG is increased, as shown in Fig. 1E. We found that expression of genes encoding enzymes involved in the TCA cycle are also downregulated (Fig. S1C). Expression of malate dehydrogenase, fumarase and citrate synthase 1 are significantly downregulated. This suggests that large-scale remodeling of central carbon metabolism is a component of the response to N-limitation in *C. sorokiniana*.

Inhibition of TOR kinase leads to decreased fatty acid biosynthesis, similar to N-limitation

The relationship between TOR signaling and N-metabolism is well established in the budding yeasts

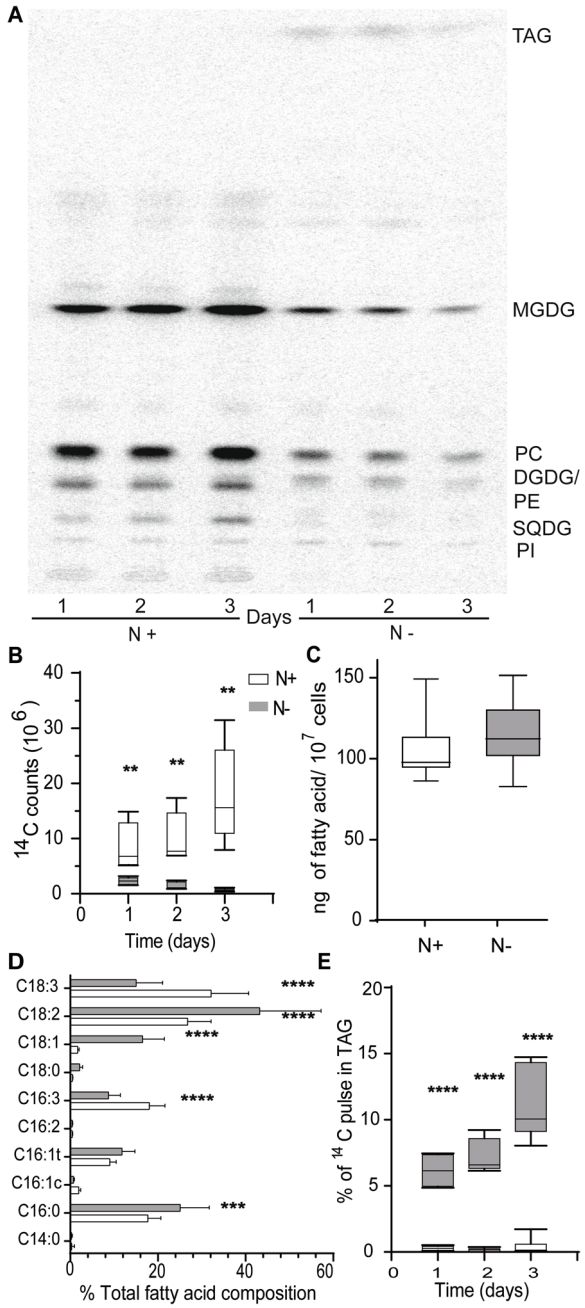

Fig. 1 Downregulation of fatty acid under nitrogen starvation in *C. sorokiniana*. **A** TLC- autoradiograph of 10^7 *C. sorokiniana* cells grown in N replete (N +) and deplete (N-) media fed with ^{14}C acetate after 1, 2, and 3 days of inoculation. **B** Quantitative measurement of ^{14}C acetate incorporated into fatty acids under nitrogen replete (N +) and deplete (N-). **C** Total Fatty Acid content of cells under nitrogen replete and deplete conditions as normalized by number of cells. **D** Percent fatty acid composition of cells under nitrogen replete and deplete conditions. **E** Percentage of ^{14}C acetate incorporated into TAG under nitrogen replete. * indicate the statistical significance of student t test $n = 9$. Error bars indicate SD

Saccharomyces cerevisiae and the fission yeast *Schizosaccharomyces pombe*. Deletion of TOR2 in fission yeast leads to N-limitation like responses [29]. The same is true of seed plants, including *Arabidopsis thaliana*, in which N-limitation has been shown to regulate TOR activity [30]. The transcriptome of *C. sorokiniana* under N-limitation also showed that the expression of RAPTOR1, a TOR complex component, is doubled (Fig. 2A). This observation and prior studies in other organisms prompted us to hypothesize that the activity of the TOR complex could be altered under N-limitation in *C. sorokiniana.*

TOR signaling is known to affect lipogenesis via the SREBP1 pathway in humans [31]. In *Saccharomyces cerevisiae*, TORC1 regulates lipid droplet formation through transcription factors such as Gln3p, Gat1p, Rtg1p, and Rtg3p [32]. Furthermore, Imamura et al. have shown that inhibition of TOR induces TAG accumulation in the microalga *Cyanidioschyzon merolae* [25]. This indicates that TOR signaling affects lipid metabolism in a number of organisms that are evolutionarily divergent, so we asked if downregulation of fatty acid synthesis under N-limitation is mediated by altered TOR signaling in *C. sorokiniana*. Li et al. have observed that rapamycin does not inhibit the growth of *C. sorokiniana* [33]. We decided to use Torin 1, a known competitive inhibitor of ATP binding of TOR kinase [34]. Unlike Li et al., we observed that Torin 1 inhibits growth of *C. sorokiniana* (Fig. S2). This shows that TOR signaling is likely essential for growth of *C. sorokiniana*. 5 and 10 μM of Torin 1 resulted in comparable growth inhibition (Fig. S2) and hence we decided to use 5 μM for further studies to minimize off-target effects.

When cells were fed ^{14}C-acetate after 4 h of treatment with 5 μM Torin 1 in N-replete media, we see that acetate incorporation into fatty acid is significantly decreased in comparison to the control cultures (Fig. 2B, C). Control cultures were cells grown in N-replete media without Torin 1. 4 h after Torin 1 treatment was chosen for the assay to avoid the effect of growth inhibition on fatty acid synthesis. Decreased fatty acid synthesis when TOR kinase activity is inhibited by Torin 1 indicates that TOR controls fatty acid synthesis in *C. sorokiniana.* We analyzed the total fatty acid content of the cells treated with Torin 1 and rapamycin and did not observe any change in the composition at 2 and 24 h after inhibition (Fig. S3).

N-limitation alters TOR signaling

To further understand the mechanism of TOR mediated regulation of fatty acid metabolism, and relationship between TOR signaling and N-limitation, we performed a quantitative proteomic and phosphoproteomic analysis of cultures grown under these

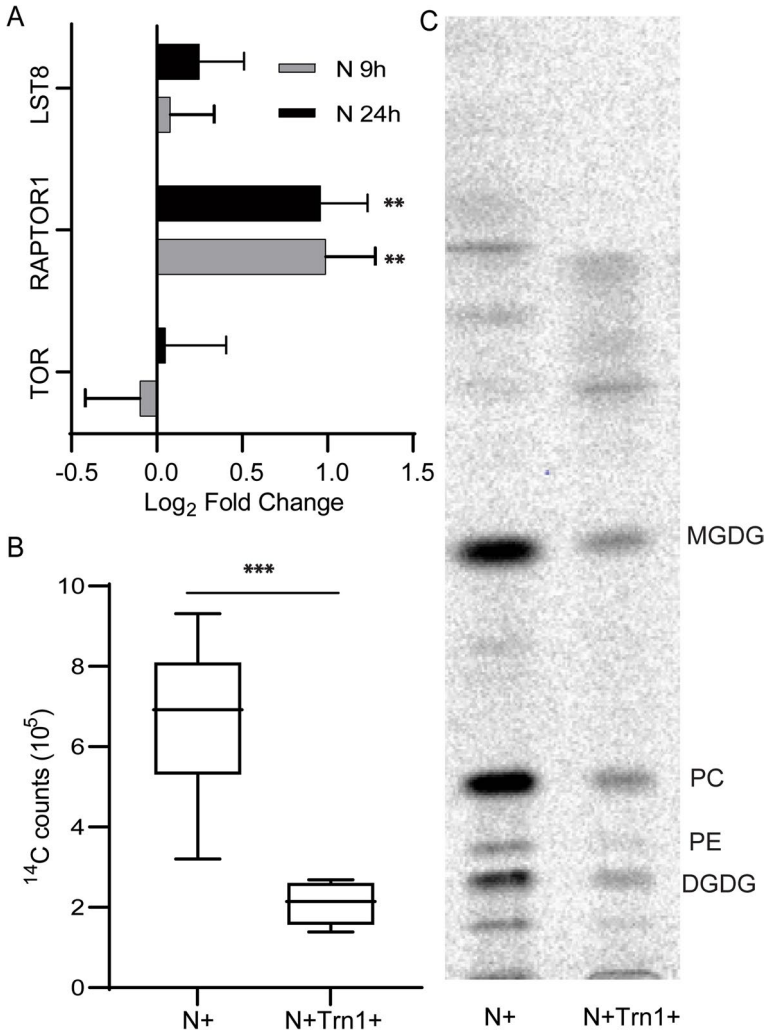

Fig. 2 Control of fatty acid synthesis under nitrogen limitation by TOR. **A** Expression levels of different known TOR complex members under nitrogen limitation conditions. **B** TLC- autoradiograph of C. sorokiniana cells fed with ^{14}C -acetate to track de novo fatty acid synthesis grown in N replete media with (N + Trn1 +) or without (N +) TOR inhibitor- torin1 **C**). Quantitative measurement of ^{14}C -acetate incorporation into fatty acid as a measure of de novo fatty acid synthesis when fed with (N + Trn1 +) or without (N +) Torin1. * indicate the statistical significance of student t test $n = 9$. Error bars indicate SD

conditions. *C. sorokiniana* cultures were grown in N-replete and -limited conditions. Twenty-two hours after inoculation, an aliquot of N-replete culture was diluted to 10^7 cells/ml and Torin 1 was added to a final concentration of 5 µM. Cultures with Torin 1 were incubated for 90 min before pelleting for sample preparation. N-limited and -replete cultures were harvested 24 h after inoculation. N-replete samples were used as control for both Torin 1 treated and N-limited samples. This shorter period for Torin 1 treatment was chosen arbitrarily to allow for the activation of autophagy and other direct targets of TOR kinase yet decrease the effect of cell cycle inhibition and other downstream effects on the data generated.

A total of 3424 proteins were identified of which 3237 were identified with at least ≥ 2 peptides and quantified across the three treatments. These proteins have a molecular weight ranging from 4–634 kDa. Changes in abundance were calculated, with a fold-change of 0.5 and lower considered downregulated, and 1.5 and above as upregulated, with a p-value < 0.05. The abundance of 299 and 133 proteins decreased in N-limited and Torin 1 treated samples, respectively, while 52 proteins decreased in abundance in both conditions as shown in Fig. 3A. This accounts for 17% of the total proteins downregulated in N-limitation and 39% for Torin 1 treatment. Hypergeometric probability analysis shows a significant overlap with a representation factor of 4.5 ($p < 7.144e\text{-}23$).

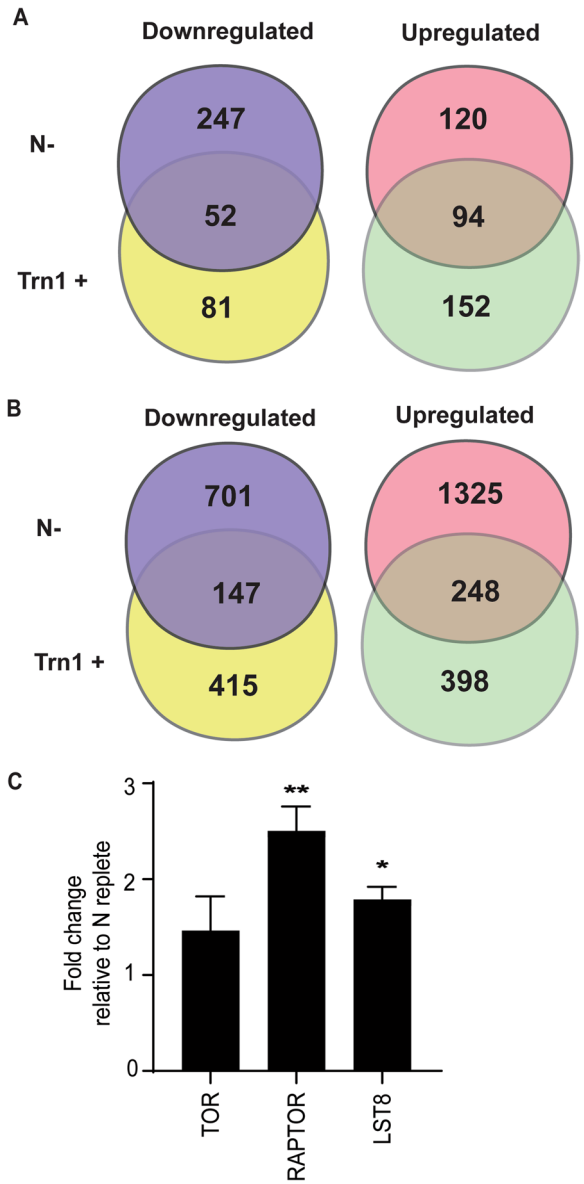

Fig. 3 TOR signaling is affected under nitrogen limitation. **A** Venn diagram showing the number of proteins that are differentially regulated under nitrogen limitation (N-) and torin1 treatment (Trn1 +). Fold change is relative to control (N replete) cutoff, ≤ 0.5and ≥ 1.5. *p*-value ≤ 0.05 or less ($n = 3$). **B** Venn diagram showing the number of phosphopetides that are differentially regulated under nitrogen limitation and torin1 treatment. Fold change relative to control (N replete) cutoff, ≤ 0.75and ≥ 1.5. *p*-value ≤ 0.05 or less. ($n = 3$), **C** Fold change in the protein level of TOR kinase, RAPTOR and LST8 under nitrogen limitation relative to control (N replete). *indicate *p*-value significance ($n = 3$)

Similarly, the abundance of 214 and 246 proteins increased in N-limited cells and Torin 1 treated samples respectively (Fig. 3A) and 94 proteins in both conditions which amounts to 44% of proteins in the N-limited condition. (Representation factor: 6.1; $p < 1.305e\text{-}56$).

A total of 6477 unique phosphopeptides belonging to 1985 proteins were detected in the phosphoproteomic analysis. Figure 3B indicates the number of peptides whose phosphorylation status was significantly ($p < 0.05$) decreased under N-limitation and Torin 1 treatment, with fold change cutoffs of ≥ 1.5 and ≤ 0.5 for N-limited samples and ≥ 1.5 and ≤ 0.75 Torin 1 treatment. The less stringent cutoff for the Torin 1 treatment comparison was chosen to account for the shorter incubation period of 90 min, versus the 24-h N-limitation treatment. 848 phosphopeptides belonging to 549 proteins had decreased phosphorylation levels under N-limitation, while Torin 1 treatment affected 562 phosphopeptides belonging to 402 proteins. 147 phosphopeptides were commonly dephosphorylated under both conditions which is 17% of peptides in N-limitation samples whose phosphorylation is decreased (Representation factor: 2.0; $p < 1.632e\text{-}18$). 1573 peptides had increased phosphorylation under N-limitation and 248 of these peptides were common between Torin 1 treated cells and N-limited cells (Fig. 3B) (Representation factor: 1.6; $p < 2.636e\text{-}17$). There is a substantial and statistically significant overlap of proteome and phosphoproteome between N-limitation and TOR inhibition, indicating that TOR activity is affected under N-limitation. We tabulated the phosphorylation status of *C. sorokiniana* orthologs of known targets of the TOR complex in Arabidopsis, as reported by Van Leene et al. [35] (Table 1 & supplement file). We observe that proteins such as S6K, ATG18, eIF2B-δ1, eIF4G, YAK1, ATG1 and, RPS6A have at least one site that is differentially phosphorylated. Some of these phosphosites are similarly phosphorylated under N limitation and Torin 1 treatment. Decreased phosphorylation of these sites in Torin 1 treated samples indicate that Torin 1 does inhibit TOR activity in *C. sorokiniana*.

Protein levels of known TOR complex members, RAPTOR and LST8 are increased in nitrogen starved cells (Fig. 3C). It should be noted that the increase in RAPTOR level is coupled to an increase in the expression of the gene, indicating that this process is transcriptionally controlled. With the available data, we are unable to speculate how this affects the functioning of the complex. We also observed differential phosphorylation of RAPTOR and TOR kinase (Table 2). In TOR kinase, T1195 and S1581 were hyperphosphorylated while S1209 and S2439 were hypo phosphorylated. S2439 is in a motif pSppr. This motif is adjacent to the catalytic domain and conserved in many different algae (Fig. 4). This serine is found to be phosphorylated in *C. reinharditii* as well [23]. Further, we observed that S504, S510, S514, S521 and S523 of RAPTOR were hypophosphorylated under N limitation. These residues are in TOR-interacting FAT domain. The effect of these phosphorylations

Table 1 Known targets TOR signaling. A select list of known targets of TOR kinase in Arabidopsis. Ratios of 0.01 and 100 are arbitrary fold changes to indicate that the peptides are not detected in the treated conditions and in control samples, respectively. *N.D* Not Detected in the quantitative proteome. [a]indicates statistical significance

Prot-ein	Arabidopsis homolog(s)	Peptide [position in protein]	Degree of Modification [position (probability)]	Fold change in phosphorylation		Fold change in protein abundance	
				N- lim	Torin1	N- lim	Torin1
S6K	AT3G08730 (S6K1), AT3G08720 (S6K2)	SIESIDNFDK [497-506]	1x [S4 (100)]	0.01[a]	0.546	ND	ND
ATG18	AT1g03380 (ATG18G), AT1G54710 (ATG18H), AT5G4730 (ATG18F)	NLYAGQLADVEPI-AAAFLPSGPGSPK [620-645]	1x [S24 (100)]	100[a]	100[a]	100	ND
eIF2B-δ1	AT5G38640, AT2G44070, AT1G48970	VEGATPSPR [19-27]	1x [S7 (100)]	0.01[a]	0.831	1.47	1.181
		ATPVGASPPGGR [115-126]	1x [S7 (100)]	0.351	0.853		
		AGGPPATPPSVSSGP-SASGSAELPPIR [68-94]	1x [S20 (100)]	0.598	0.66		
		AGGPPATPPSVSSGP-SASGSAELPPIRTDSSK [68-99]	1x [T/S]	0.574	0.917		
		DTSLADAGAASTVTGSP-SPVIIPPAFAGQSR [28-58]	1x [T/S]	0.323	0.672		
		TLPLTPVGTSAPADLG-GQFASAADDSPRV-VQQHAPEAGAP-SAAQAAGK [127-174]	2x [T1 (98.9); S26 (98.9)]	0.01[a]	0.881		
eIF4G	AT3G60240 (eIF4G), AT5G57870	TGSGRGPPAPPAR [1349-1361]	1x [S3 (100)]	0.52	0.81	0.86	0.883
		GPESHPIPNGTPSPPPEP-AAPGGMSWAAR [41-69]	1x [T11 (99.3)]	0.01[a]	0.928		
		GPESHPIPNGTPSPPPEP-AAPGGMSWAAR [41-69]	1x [T/S]	0.01[a]	0.479		
		EAAAQEAP-SEAAAPAAASESSFAAK [701-725]	2x [S20 (99.3); S21 (99.3)]	0.096	0.917		
		EAAAQEAP-SEAAAPAAASESSFAAK [701-725]	1x [S18 (100)]	0.251	0.802		
YAK1	AT5G35980 (YAK1)	TSGTLPHQSSAFSSYSPPER [2-21]	1x [S16 (100)]	0.01[a]	0.878	ND	ND
ATG13	AT3G49590 (ATG13)	GSSGAEAPPSPSPPTAR [511-527]	1x [S/T]	0.303	0.51	ND	ND
RPS6A	AT4G31700 (RPS6A), AT5G10360 (RPS6B),	VQVLMSPGDQCFR [73-85]	1x [S6 (100)]	0.33	0.92	ND	ND

on the kinase activity and protein–protein interactions are beyond the scope of this work, however we hypothesize that these modifications affect the functioning of the TOR complex. Conservation of the pSppr motif near the C-terminus of the TOR-kinase in different algal lineage raises the possibility that TOR activity could be controlled by differential phosphorylation of this residue by a conserved kinase whose identity is yet unknown.

Robust and statistically significant similarity between the proteome and phosphoproteome under N-limitation and Torin 1 treatment, similar trend in phosphorylation of known targets of TOR signaling and changes in the phosphorylation status of TOR complex components in the N-limited condition suggest that TOR signaling is altered under N- limitation.

Effect of N-limitation and TOR inhibition on ACCase and FAS complex components

We observed that protein levels of the carboxyltransferase component of the plastidic ACCase complex is decreased under both N-limitation and TOR inhibition (Fig. 5A). 3-oxoacyl-ACP reductase of the FAS complex is also significantly downregulated under N-limitation (Fig. 5B). We hypothesize that these changes in

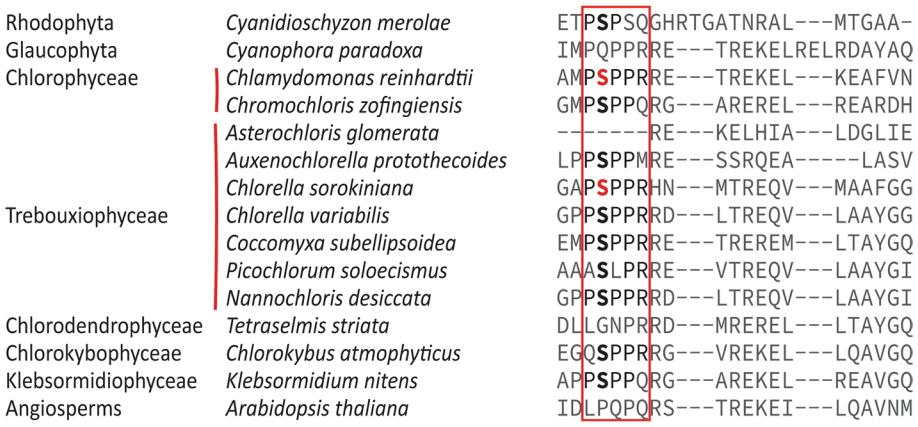

Fig. 4 Conservation of pSppr motif in TOR kinase of different microalgae. Multiple sequence alignment of TOR kinase protein from different microalgae highlighting (red box) the conserved pSppr motif in the C-terminus. Serine in red indicates known phosphorylation of the residue

Table 2 Phosphorylation status of TOR complex proteins. Ratios of 0.01 and 100 are arbitrary fold changes to indicate that the peptides are not detected in the treated conditions and in control samples, respectively. *N.D.D* No Domain Detected. [a]indicates statistical significance

Position in Protein	Sequence	Degree of phosphorylation	Phosphorylated amino acid (probability)	Abundance Ratio: (N-) / (N+)	Predicted domain
TOR kinase (2451 aa)					
1192-1202	QSTPDRLHLER	1xPhospho	T1195 (99.3)	16.656[a]	N.D.D
1203-1218	TVTMASDEAGLNTGL	1xPhospho	S1209 (100)	0.571	N.D.D
1569-1599	WEEEEEAGGRGSPDGGLTPSS-LLAGGLGGAR	1xPhospho	S1581 (100)	100[a]	FAT- domain (IPR014009)
2434-2441	TGAPSPPR	1xPhospho	S2439 (100)	0.231	Pi3-/4- kinase, catalytic domain (IPR000403)
RAPTOR (1786 aa)					
499-516	SVPSATSAPGSAAGSIGR	3xPhospho	S506 (100); S510 (100); S514 (100)	0.01[a]	FAT
		1xPhospho	S514 (100)	0.493	
		2xPhospho	S510 (100); S514 (100)	0.518	
517-530	VGSSGSIAGSGVLR	3xPhospho	S520 (100); S521 (100); S523 (100)	0.01[a]	FAT
		2xPhospho	S520 (100); S523 (100)	0.145[a]	
		1xPhospho	S520 (100)	1.016	
810-858	ESAAYGEPRPLSAQGSGG-SLDAYAASAAAAGHAAAAAL-PPSGIYTASCR	1xPhospho	S/Y/T	100[a]	N.D.D

the protein levels affect the rate of fatty acid synthesis. It should be noted that the expression of many genes encoding FAS complex members are downregulated under N-limitation, but the protein levels do not follow the pattern. We did not observe any phosphorylation of plastidial-ACCase or FAS complex members. Nevertheless, reduction in protein levels of a core component of the ACCase and of 3-oxoacyl-ACP reductase (FAS) would be expected to decrease the rate of fatty acid synthesis. Additionally, in a transcriptomic study of *C. sorokiniana* cells treated with the TOR kinase inhibitor AZD8055, Li et al. observed that the expression of all FAS complex members are downregulated [33]. This indicates that TOR controls fatty acid synthesis at both the transcriptional level, and in regulating protein abundance via changes in translation or protein turnover.

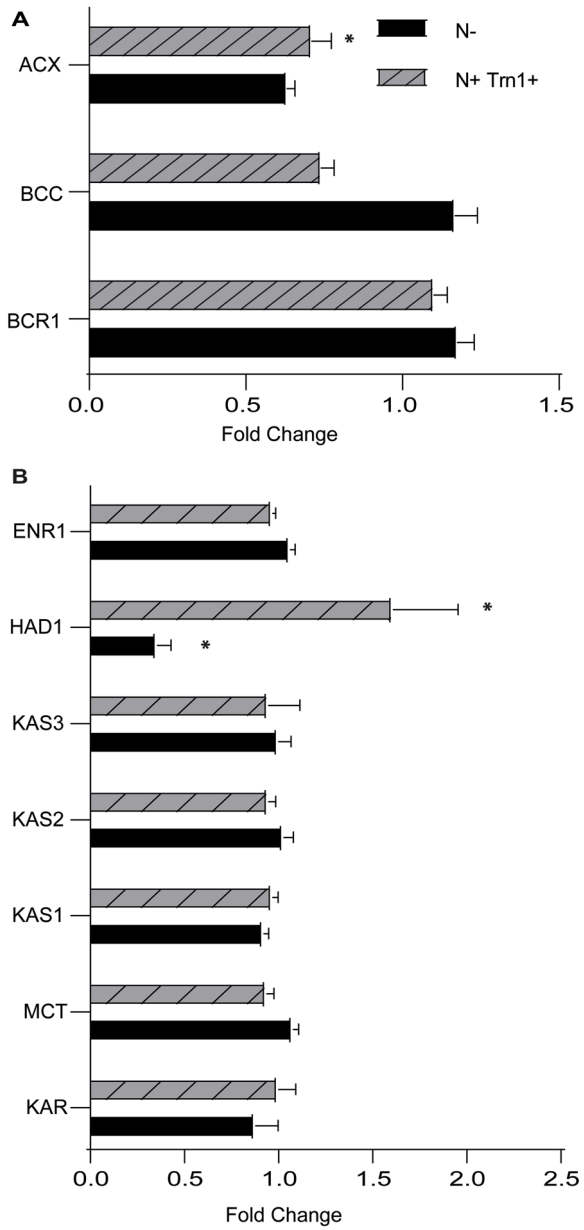

Fig. 5 Protein levels of ACCase and FAS complex members. **A** Protein levels of different components of ACCase complex members under nitrogen limitation (N-) and Torin 1 treatment (N + Trn1 +). BCR1: Biotin carboxylase, BCC: Acetyl-CoA biotin carboxyl carrier protein, ACX: Carboxyltransferase. **B** Protein levels of different enzymes involved in the process of fatty acid synthesis. KAR: 3-Oxoacy-ACP reductase, MCT: Malonyl-CoA: ACP transacylase, KAS: 3-Ketoacyl-ACP-synthase, HAD: 3-Hydroxyacyl-ACP dehydratase, ENR: Enoyl-[acyl carrier protein] reductase. Error bars indicate SD ($n = 3$)

TOR mediated regulation of fatty acid synthesis under N-limitation in *Chlamydomonas* reinhardtii

C. sorokiniana and the well-studied model microalgae *C. reinhardtii* are members of the taxa Chlorophyta. Therefore, we enquired if similar mechanisms of TOR-signaling mediate control of fatty acid synthesis under N-limitation in *C. reinhardtii.* For this, we first queried the published transcriptome of *C. reinhardtii* under N-limitation [36] and found that expression of all the genes encoding components of the plastidic ACCase and FAS complexes were downregulated as early as 4 h after inoculation in nitrogen limited media (Fig. S3A, B). This indicates that there is indeed a transcriptional mechanism for downregulation of fatty acid synthesis under N-limitation. Next, we took advantage of the RNAseq data published by Kleessen et al. to investigate if inhibition of TOR activity by rapamycin affects the transcript levels of these genes [37]. While the expression of genes encoding BCC1, BCC2, KAS2, and KAS3 decrease to a very small extent, we see that BCR1 and KAR1 expression decreases by half after 4 h of rapamycin treatment (Fig. S3C, D). Thus, TOR inhibition affects fatty acid synthesis at a transcriptional level in *C. reinhardtii*, similar to *C. sorokiniana*. To query if the transcriptional downregulation of these genes indeed affect fatty acid synthesis in *C. reinharditii* under N-limitation or TOR inhibition, we carried out a ^{14}C- acetate labeling experiment. We used either 5 µM Torin 1 or 1 µM rapamycin to inhibit TOR activity. Incorporation of ^{14}C- acetate was significantly decreased under N-limitation and Torin 1 treatment (Fig. 6A, B), thus indicating that TOR-mediated control of fatty acid synthesis under N-limitation is conserved between *C. sorokiniana* and *C. reinhardtii.*

Discussion

Downregulation of fatty acid synthesis under N-limitation

Our study shows that the rate of fatty acid synthesis is decreased under N-limitation in the green algae *C. sorokiniana* and *C. reinhardtii*. This indicates that carbon flux into fatty acid synthesis is decreased during N-limitation in the green algal lineage. This information is crucial for any future biotechnological interventions to increase TAG accumulation in these organisms. This also raises the question, if inducing N-limitation-like conditions would be a means for channeling photosynthate to fatty acid, and in turn into oil production. Further, any strategy for enhancing oil production via the N-limitation response will have to account for the fact of decreased fatty acid synthesis under these conditions.

Nitrogen starvation mediated downregulation of fatty acid synthesis is conserved in the yeast *Saccharomyces cerevisiae.* In *S. cerevisiae,* under N-limitation, reduction

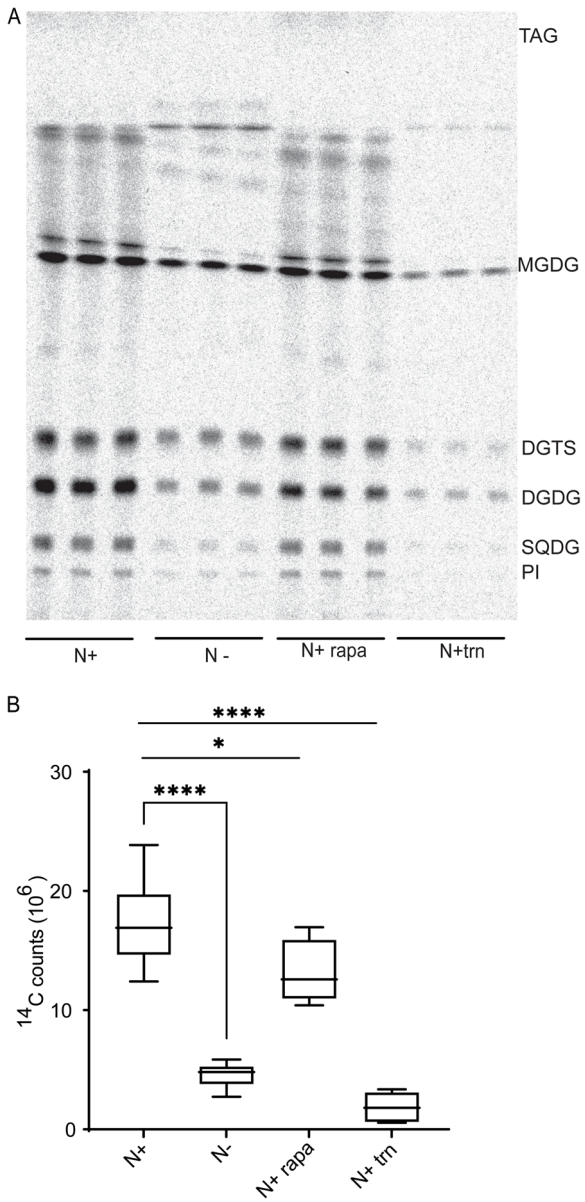

Fig. 6 Regulation of fatty acid synthesis in *Chlamydomonas reinhardtii* under nitrogen limitation and TOR inhibition. **A** TLC- autoradiograph of *C. reinhardtii* cells grown in N replete (N+), limited (N-), nitrogen replete with rapamycin (N+rapa) or torin1 (N+trn) fed with ^{14}C acetate to track de novo synthesized fatty acid. **B** 14C-counts in fatty acid under nitrogen replete (N+), nitrogen deplete (N-), nitrogen replete with rapamycin (N+rapa) and torin1 (N+trn+). * indicate *p*-value confidence (student t-test)

in fatty acid synthesis is achieved by autophagy dependent specific degradation of FAS components [38]. Prevention of FAS degradation decreased the viability under N-limitation. This indicates that *S. cerevisiae,* much like *C. sorokiniana* and *C. reinhardtii* actively decreases fatty acid synthesis under N-limitation. Conservation of decreased de novo fatty acid synthesis under N-limitation in evolutionarily diverse organisms, like microalgae and yeast, indicates that this is an essential adaptive response. When growth rate and cell division are limited by N-limitation, the demand for membrane glycerolipids will likewise be lower. When demand for membrane glycerolipids, a major sink for fatty acids, is lower, it would make sense for the cells to decrease the production of fatty acids. Further, fatty acid synthesis is an energy intensive process consuming NADPH and ATP molecules [14]. Decreasing carbon flux through this pathway would save energy (ATP) and reducing equivalents (NADPH). It is unclear if this is the only reason for the downregulation.

TOR signaling under N-limitation

TOR signaling is an integral part of energy and nutrient sensing in eukaryotes. This is common to yeast, mammals, and plants [39]. Multiple lines of evidence suggest the involvement of TOR signaling under N-limitation in microalgae. When treated with rapamycin under N-replete conditions, *C. reinhardtii* cells accumulate various amino acids within the first 5 min [40]. This accumulation of amino acids is not from increased proteasomal activity but from active acquisition of nitrogen from the media via the activity of glutamine synthase (GS) and glutamine-2-oxoglutarate- aminotransferase. This active acquisition of nitrogen from the media is similar to an N-starvation response. Additionally, Mallen-Ponce et al., have shown that TOR activity is controlled by CO_2 assimilation and this in turn controls the levels of certain amino acids in Chlamydomonas [21]. In a phosphoproteomic analysis of nitrogen starved cells of *C. reinhardtii*, Roustan et al. identified differential phosphorylation of ATG13, NNK1 and RSP6, known targets of TOR signaling [41]. This indicates that N-utilization/limitation and TOR signaling are linked in *C. reinhardtii*. Our work shows that under N-limitation in *C. sorokiniana*, there is a change in the abundance of individual proteins of the TOR complex (RAPTOR and TOR kinase) and differential phosphorylation of TOR kinase and RAPTOR. This coupled with significant overlap between the changes in the quantitative proteome and phosphoproteome under N-limitation and in TOR-inhibited cells indicates that TOR signaling is indeed affected under N-limitation. The relationship between TOR signaling and N-availability is not limited to microalgae. In Arabidopsis, nitrogen starvation leads to inactivation of TOR kinase and supplementation of select amino acids or inorganic nitrogen activates TOR kinase [30]. In mammalian cells and *Saccharomyces cerevisiae,* TOR activity is controlled by amino acid availability via GTPases, RAB(A-D), and GRT1/2, respectively. Further, as mentioned earlier, in

the fission yeast, *Schizosaccharomyces pombe,* deletion of TOR2 mimics nitrogen starvation [29].

It is not surprising that TOR signaling is controlled by N-availability in a variety of eukaryotes ranging from yeast and microalgae to land plants, since TOR functions as a central node in assimilating growth cues such as hormones and various nutrient availability [42], and nitrogen is an important macronutrient that regulates growth.

TOR mediated regulation of fatty acid synthesis

In this study, we show that inhibition of TOR activity leads to a decrease in fatty acid synthesis thereby linking fatty acid synthesis to TOR signaling in the green plant (*Viridiplantae*) lineage. While there are transcriptional (Li et al., 2022) and protein level changes of ACCase and FAS complex members (this study), it is unclear if these are the only means by which TOR regulates fatty acid synthesis. It is also possible that TOR regulates the flux of carbon flow into the TCA cycle, in addition to the transcriptional and post-translational control of ACCase and FAS.

In mammalian systems, TORC1 regulates fatty acid synthesis at the transcriptional level by regulating SREBP1, a transcription factor that controls the expression and activities of ACCase and FAS complexes [31]. It is interesting to note that TOR regulates fatty acid synthesis at the transcriptional level in evolutionarily distant organisms, such as mammals and microalgae. Evolutionary conservation of TOR mediated control of fatty acid synthesis can be attributed to two factors: TOR is a central regulator of metabolism that responds to many stress conditions such as nutrient limitation [43], and fatty acid biosynthesis is a major sink for carbon and reducing equivalents. As mentioned earlier, decreasing fatty acid synthesis under nutrient limitation is in line with cellular needs under these stress conditions. TOR, being a central regulator of metabolism, coordinates the fatty acid synthesis process in response to external cues.

Knowledge of TOR functioning in the plant lineage has been lagging in comparison to that of mammalian and yeast cells, however in the past decade, the role of TOR kinase signaling as coordinator of metabolism in the green lineage has become clear [17, 20, 42, 44–48]. Our current work adds to the list of metabolic processes that are controlled by TOR signaling.

Conclusion

In this work we have presented evidence to show that under N-limitation, microalgae like *C. sorokiniana* and *C. reinhardtii* reduce their rate of fatty acid synthesis, and that this downregulation is likely mediated by signal processing and transduction via the TOR kinase complex. This information will be useful in engineering microalgae to produce triacylglycerols and other storage compounds under nutrient replete growth conditions and may provide new insights into TOR-mediated control of fatty acid synthesis in land plants.

Methods

Growth and N-limitation of *C. sorokianiana* and *C. reinhardtii*

C. sorokianiana and *C. reinhardtii* were grown in Tris Acetate Phosphate (TAP) media under continuous light with shaking (200 rpm). *C. sorokiniana* was grown at 25 °C while *C. reinhardtii* was grown at 22 °C. TAP media was prepared as described by Gorman and Levine [49]. In nitrogen deplete media (TAP-N), final concentration of ammonium chloride was 250 µM. For nitrogen starved cultures, parent cultures were grown for 2 days and washed thrice in appropriate media (TAP or TAP-N). The cultures were inoculated at a final concentration of 10^7 cells/ml for *C. sorokiniana* and 5×10^6 cells/ml for *C. reinhardtii*.

Lipid extraction and total fatty acid assay

Lipid extraction was carried out using the Bligh and Dyer method [50]. Glycerolipids were sequentially separated by Thin Layer Chromatography (TLC) on silica-G60 plates (EMD-Millipore) in a two-stage solvent system. First, the plate was developed for ~ 2/3 of its length in chloroform, methanol, acetic acid, and water (85:12.5:12.5:3) to separate polar lipids. Next, the plate was dried and developed for the full length in petroleum ether, diethyl ether and acetic acid (80:20:1) to separate nonpolar lipids (triacylglycerol). For total fatty acid analysis, lipids extracted from 10^7 cells were transesterified in methanolic HCl for 30 min at 80 °C to form Fatty Acid Methyl Esters (FAME). FAMEs were extracted into hexane by adding 1 ml hexane and 1 ml of 1 mM NaCl. The hexane phase was concentrated under a stream of nitrogen and quantified using GC-FID with Innowax column as previously described [51]. 15:0 fatty acid was used as internal standard for quantification.

^{14}C acetate labeling to measure de novo fatty acid synthesis

To measure *denovo* fatty acid synthesis, we carried out ^{14}C- acetate feeding experiments. Cells were grown in appropriate growth conditions (N + and N-) and then washed thrice in media lacking acetate (TP or TP-N) to remove any remaining acetate. Cells were then diluted to equal number of cells (10^7 cell for *C. sorokiniana* and 5×10^6 for *C. reinhardtii)* in 1 ml of TP / TP-N/ TP + Torin 1/ TP + rapamycin and 10^5 cpm of ^{14}C acetate (specific activity of 56 mCi/mMol- supplied by ARC Inc.) was added and incubated for 45 min. After 45 min the

cells were washed thrice in appropriate media to remove any remaining ^{14}C acetate. Lipid extraction and lipid separation was carried out as mentioned earlier. After drying, the TLC plates were exposed to a phosphoimager screen for 24 h, and counts were read on a GE-Typhoon FLA 9500 scanner. Images were analyzed by ImageQuant TL v8.1. Total fatty acid level in each sample was calculated as a sum of all lipids in a given TLC lane.

Inhibition of TOR signaling

In *C. sorokiniana* TOR activity was inhibited with 5 μM Torin 1 (EMD Millipore Corp.,). In *C. reinhardtii,* TOR kinase was inhibited using 1 μM rapamycin (Sigma Aldrich) or 5 μM Torin 1. To assay the effect of TOR inhibition on fatty acid synthesis, we incubated either *C. sorokiniana* or *C. reinhardtii* in TAP media with or without the inhibitors for 4 h, and then labeled with ^{14}C- acetate as described above.

Protein preparation

For proteomic studies, samples were grown, treated, and collected as described (see results). Three replicates per condition were used for each treatment group. Protein samples for quantitative proteomic and phosphoproteomic analyses were prepared as follows: cells were ruptured by bead beating in lysis buffer (50 mM Tris-pH 8.0, 1 mM DTT, 0.5 mM PMSF and 2 × PhosStop EASYpack-Roche) for 7 cycles with 30 s of beating at 400 rpm and 45 s on ice for each cycle. Glass beads of 0.5 mm diameter were used. Following the rupture, cells and debris were separated by spinning at 3000 rpm for 5 min at 4 °C.

Proteins were precipitated and washed using the ProteoExtract™ Protein Precipitation Kit (MilliporeSigma, Burlington MA) and then redissolved in 8 M Urea, 0.2 M tris–HCl, pH 8.5 containing 2 × PhosSTOP™ phosphatase inhibitor (Roche, Basel, Switzerland), 1 × cOmplete™, EDTA-free Protease Inhibitor Cocktail (Roche) and 10 mM DTT. Protein amounts were quantified using the CB-X™ protein assay (G-Biosciences, St Louis, MO). 1 mg of each sample was reduced at 37 °C for 1 h and then alkylated with 20 mM iodoacetamide (20 min at RT in darkness), then quenched with an equimolar amount of DTT. Samples were diluted to 4 M urea with water and digested with 10 μg Lys-C (1:100 enzyme:substrate) at 37 °C for 4 h. The urea was then diluted to 1 M by addition of 0.1 M tris–HCl, pH 8.5 and trypsin digestion carried out for 16 h at a ratio of 1:100. A further aliquot of trypsin (1:100) was added and digestion was carried out for a further 3 h. Digests were acidified with 20% TFA to pH 3, then desalted using 100 mg Sep-Pak® C18 reverse-phase SPE columns (Waters Corp, Milford, MA). Eluted samples were dried down and redissolved in 50 mM TEAB. A portion was set aside for analysis of the complete digest sample.

Phosphoenrichment

For each sample, 0.75 mg of digested, desalted, dried peptide was dissolved in 2 M lactic acid, 60% acetonitrile, 0.3% TFA to 3 mg/mL and shaken vigorously with TiO_2 beads (Titansphere, 5 μm, GL Sciences, Tokyo, Japan) in a ratio of 1:5 sample: beads (w/w) for 20 h at 4 °C. The beads were then washed with 3 × 100μL of the lactic acid binding solution and finally resuspended in 50μL and placed into 200 μL tips (Eppendorf, Hauppauge, NY) plugged with 2 layers of 3 M™ C8 Empore™ membrane (ThermoFisher Scientific, Waltham, MA). For each sample, 100 μL of the same solution was spun through the beads at 3000 × g 3 times. The beads were then further washed with 3 × 200μL of 80% acetonitrile, 0.4% TFA at 3000 × g. Bound phosphopeptides were then eluted 3 times with 100 μL ammonium hydroxide (5% v/v) into 1.5 mL Lo-Bind tubes (Eppendorf). These were then frozen and lyophilized. A 2nd elution of phosphopeptides was performed using 3 × 100 μL pyrrolidine (5% v/v) at 1000 × g and the samples were frozen and lyophilized. Both eluates for each sample were pooled and desalted using an Oasis μElution plate (Waters Corp), dried down and then redissolved for analysis by LC–MS/MS.

LC–MS/MS analysis of the proteome and phosphoproteome

Peptide and phosphopeptide samples were analyzed by LC–MS/MS on an RSLCnano system (ThermoFisher Scientific) coupled to a Q-Exactive HF mass spectrometer (ThermoFisher Scientific). The samples were first injected onto a trap (Acclaim PepMap™ 100, 75 μm × 2 cm, ThermoFisher Scientific) for 2.8 min at a flow rate of 5 μL/min, 1.5% acetonitrile, 0.2% formic acid before switching in-line with the main column. Separation was performed on a C18 nano column (Acquity UPLC® M-class, Peptide CSH™ 130A, 1.7 μm 75 μm x 250 mm, Waters Corp) at 260 nL/min with a linear gradient from 5–32% over 96 min. The LC aqueous mobile phase contained 0.1% (v/v) formic acid in water and the organic mobile phase contained 0.1% (v/v) formic acid in 80% (v/v) acetonitrile. Mass spectra for the eluted peptides were acquired on a Q Exactive HF mass spectrometer in data-dependent mode using a mass range of m/z 375–1500, resolution 120,000 for the MS1 peptide measurements. Data-dependent MS2 spectra were acquired by HCD fragmentation with a normalized collision energy (NCE) set at 28%, AGC target set to 1×10^5, 15,000 (for phosphopeptides at 30,000) resolution, intensity threshold 1×10^5 and a maximum injection time of 118 ms (86 ms for phosphopeptides). Dynamic exclusion was set at 45 s

for the complex digest and 30 s for the phosphopeptide analysis to help capture phospho isomers.

Data analysis

Data were analyzed in Proteome Discoverer 2.2 software (ThermoFisher Scientific) and searched using Mascot 2.6.2. The databases searched were the common contaminants database cRAP (116 entries, www.theGPM.org) and in-house *Chlorella sorokiniana* gene catalog with13,906 entries. Gene identifiers and sequence data used for the analysis are available at NCBI under BioProject PRJNA34632. Methionine oxidation, protein N-terminal acetylation, deamidation of glutamine, carbamidomethylation of cysteine and Ser/Thr and Tyr phosphorylation were set as variable modifications. A maximum of two trypsin missed cleavages were permitted and the precursor and fragment mass tolerances were set to 10 ppm and 0.02 Da, respectively. Peptides were validated by Percolator with a 0.01 posterior error probability (PEP) threshold. The data were searched using a decoy database to set the false discovery rate to 1% (high confidence). The localization probabilities of the PTMs were obtained using ptmRS (Taus et al. 2011). The peptides were quantified using the precursor abundance based on intensity. The peak abundance was normalized using total peptide amount. The peptide group abundances are summed for each sample and the maximum sum for all files is determined. The normalization factor used is the factor of the sum of the sample and the maximum sum in all files. The protein ratios are calculated using a pairwise ratio-based method. The protein ratios are calculated as median of all possible pairwise ratios between the replicates of all connected peptides. To compensate for missing values in some of the replicates, the replicate-based resampling imputation mode was selected. The significance of differential expression is tested using an ANOVA test which provides adjusted *p*-values using the Benjamini–Hochberg method for all the calculated ratios.

Multiple sequence alignment

TOR-kinase sequence for different algae were collected from Phycocosm [52] and Multiple sequence alignment was performed using Clustal Omega [53].

Statistical analysis

All statistical analysis for biochemical and growth assays were performed using Graphpad prism v9.

Abbreviations

N	Nitrogen
TOR	Target of Rapamycin
TAG	Triacylglycerol
ACCase	Acetyl-CoA Carboxylase
BCR1	Biotin carboxylase
BCC	Acetyl-CoA biotin carboxyl carrier protein
ACX	Carboxyltransferase
FAS	Fatty Acid Synthase
KAS	Ketoacyl-ACP-Synthase
KAR	3-Oxoacy-ACP reductase
MCT	Malonyl-CoA: ACP transacylase
HAD1	Hydroxyacyl-ACP-Dehydratase
ENR1	Enoyl Reductase
MGDG	MonoGalactosyl DiacylGlycerol
DGDG	DiGalactosyl DiacylGlycerol
PC	Phosphatidyl Choline
PE	Phosphatidyl Ethanolamine
SQDG	Sulfoquinovosyl Diacylglycerol
PI	Phosphatidyl Inositol

Supplementary Information

The online version contains supplementary material available at https://doi.org/10.1186/s12870-024-05408-7.

Supplementary Material 1. Shows the quantitative proteomic data generated in this study.

Supplementary Material 2. Shows the phosphoproteomic data generated in this study.

Supplementary Material 3. Shows the phosphorylation targets of known targets of TOR kinase in Arabidopsis.

Supplementary Material 4. Shows all the source data used to generate graphs in this article. TOR Supplement Fig 1. Expression of genes in ACCase, FAS complex and TCA cycle under N-limitation in *Chlorella sorokiniana*.

Supplementary Material 5. TOR Supplement Fig 1. Expression of genes in ACCase, FAS complex and TCA cycle under N-limitation in *Chlorella sorokiniana*.

Supplementary Material 6. TOR Supplement Fig 2. Inhibition of growth of *C. sorokiniana* by rapamycin and Torin 1.

Supplementary Material 7. TOR Supplement Fig 3. Fatty acid composition of *C. sorokiniana* cells treated with Torin 1 or rapamycin at 2 and 24 hours after treatment.

Supplementary Material 8. TOR Supplement Fig 4. Expression of gene in ACCase and FAS complex in *C. reinharditii* under N limitation or treatment with rapamycin.

Supplementary Material 9. TOR Supplement Fig 5. Unedited TLC-autoradiographs.

Acknowledgements

Not applicable.

Authors' contributions

JV conceived the hypothesis, designed, and performed the experiments and wrote the manuscript. MN and SA performed the proteomic, phosphoproteomic analysis and edited the manuscript. AM and WM performed the fatty acid analysis. NW and WRR provided critical insights and edited the manuscript.

Funding

This work was supported by National Science Foundation award number EPS-1004094 (to WRR.), NASA award number 80NSSC17K0737 (to WRR) and startup funding from the University of Nebraska-Lincoln College of Arts and Sciences and School of Biological Sciences (to WRR). The Proteomics & Metabolomics Facility (RRID:SCR_021314) and instrumentation are supported by the Nebraska Research Initiative.

Availability of data and materials

The mass spectrometry proteomics data have been deposited to the ProteomeXchange Consortium via the PRIDE [54] partner repository with

the dataset identifier PXD041691. All data in this study are available from the corresponding author upon reasonable request.

Declarations

Ethics approval and consent to participate
Not applicable.

Consent for publication
Not applicable.

Competing interests
The authors declare no competing interests.

Author details
[1]School of Biological Sciences, University of Nebraska-Lincoln, Lincoln, NE, USA. [2]Department of Biochemistry, University of Nebraska-Lincoln, Lincoln, NE, USA. [3]Center for Plant Science Innovation, University of Nebraska-Lincoln, Lincoln, NE, USA. [4]Proteomics and Metabolomics Facility, Nebraska Center for Biotechnology, University of Nebraska-Lincoln, Lincoln, NE, USA. [5]PPD, part of ThermoFisher Scientific, Henrico, VA, USA.

Received: 19 September 2023 Accepted: 11 July 2024
Published online: 06 August 2024

References

1. Hu Q, Sommerfeld M, Jarvis E, Ghirardi M, Posewitz M, Seibert M, et al. Microalgal triacylglycerols as feedstocks for biofuel production: perspectives and advances. Plant J. 2008;54(4):621–39.
2. Allen J, Black PN, Riekhof WR, Allen J, Unlu S, Demirel Y, et al. Integration of biology, ecology and engineering for sustainable algal - based biofuel and bioproduct biorefinery. 2018;5:47.
3. Beal CM, Cuellar AD, Wagner TJ. Sustainability assessment of alternative jet fuel for the U.S. Department of defense. Biomass and Bioenergy. 2021;144:105881.
4. Zhu LD, Li ZH, Hiltunen E. Strategies for Lipid Production Improvement in Microalgae as a Biodiesel Feedstock. Biomed Res Int. 2016;2016:7–9.
5. Wase N, Tu B, Allen JW, Black PN, DiRusso CC. Identification and metabolite profiling of chemical activators of lipid accumulation in green algae. Plant Physiol. 2017;174(4):2146–65.
6. Bollmeier W, Sprague S. Aquatic species program. 1989. Report No.: SERI/SP-231–3579, 5232049, ON: DE89009472. Available from: https://www.osti.gov/servlets/purl/5232049/.
7. Wase N, Black P, DiRusso C. Innovations in improving lipid production: Algal chemical genetics. Prog Lipid Res. 2018;71(July):101–23.
8. Li-Beisson Y, Thelen JJ, Fedosejevs E, Harwood JL. The lipid biochemistry of eukaryotic algae. Prog Lipid Res. 2019;74(January):31–68.
9. Li X, Moellering ER, Liu B, Johnny C, Fedewa M, Sears BB, et al. A galactoglycerolipid lipase is required for triacylglycerol accumulation and survival following nitrogen deprivation in *Chlamydomonas reinhardtii*. Plant Cell. 2012;24(11):4670–86.
10. Yoon K, Han D, Li Y, Sommerfeld M, Hu Q. Phospholipid: Diacylglycerol acyltransferase is a multifunctional enzyme involved in membrane lipid turnover and degradation while synthesizing triacylglycerol in the unicellular green microalga *Chlamydomonas reinhardtii*. Plant Cell. 2012;24(9):3708–24.
11. Chen H, Wang Q. Regulatory mechanisms of lipid biosynthesis in microalgae. Biol Rev. 2021;96(5):2373–91.
12. Vijayan J, Wase N, Liu K, Morse W, Zhang C, Riekhof WR. Reactive oxygen species mediate thylakoid membrane remodeling and triacylglycerol synthesis under nitrogen starvation in the alga *Chlorella sorokiniana*. Front Plant Sci. 2024;15.
13. Young DY, Shachar-Hill Y. Large fluxes of fatty acids from membranes to triacylglycerol and back during N-deprivation and recovery in *Chlamydomonas*. Plant Physiol. 2021;185(3):796–814.
14. Post-Beittenmiller D, Roughan G, Ohlrogge JB. Regulation of plant fatty acid biosynthesis. Plant Physiol. 1992;100:923–30.
15. Wakil SJ, Stoops JK, Joshi VC. Fatty acid synthesis and its regulation. Annu Rev Biochem. 1983;52(1):537–79.
16. Salie MJ, Zhang N, Lancikova V, Xu D, Thelen JJ. A family of negative regulators targets the committed step of de novo fatty acid biosynthesis. Plant Cell. 2016;28(9):2312–25.
17. Robaglia C, Thomas M, Meyer C. Sensing nutrient and energy status by SnRK1 and TOR kinases. Curr Opin Plant Biol. 2012;15(3):301–7.
18. Pérez-Pérez ME, Couso I, Crespo JL. The TOR signaling network in the model unicellular green alga *Chlamydomonas reinhardtii*. Biomolecules. 2017;7(3):1–13.
19. Laplante M, Sabatini DM. mTOR signaling in growth control and disease. Cell. 2012;149(2):274–93.
20. Upadhyaya S, Rao BJ. Reciprocal regulation of photosynthesis and mitochondrial respiration by TOR kinase in *Chlamydomonas reinhardtii*. Plant Direct. 2019;3(11). Available from: https://onlinelibrary.wiley.com/doi/10.1002/pld3.184. Cited 2023 Jan 18.
21. Mallén-Ponce MJ, Pérez-Pérez ME, Crespo JL. Photosynthetic assimilation of CO_2 regulates TOR activity. Proc Natl Acad Sci USA. 2022;119(2):e2115261119.
22. Mubeen U, Jüppner J, Alpers J, Hincha DK, Giavalisco P. Target of rapamycin inhibition in *Chlamydomonas reinhardtii* triggers de Novo amino acid synthesis by enhancing nitrogen assimilation. Plant Cell. 2018;30(10):2240–54.
23. Wang H, Gau B, Slade WO, Juergens M, Li P, Hicks LM. The global phosphoproteome of *Chlamydomonas reinhardtii* reveals complex organellar phosphorylation in the flagella and thylakoid membrane. Mol Cell Proteomics. 2014;13(9):2337–53.
24. Pérez-Pérez ME, Florencio FJ, Crespo JL. Inhibition of target of rapamycin signaling and stress activate autophagy in *Chlamydomonas reinhardtii*. Plant Physiol. 2010;152(4):1874–88.
25. Imamura S, Kawase Y, Kobayashi I, Shimojima M, Ohta H, Tanaka K. TOR (target of rapamycin) is a key regulator of triacylglycerol accumulation in microalgae. Plant Signal Behav. 2016;11(3):e1149285.
26. Lizzul AM, Lekuona-Amundarain A, Purton S, Campos LC. Characterization of *Chlorella sorokiniana*, UTEX 1230. Biology. 2018;7(2):1–12.
27. Bohutskyi P, Liu K, Nasr LK, Byers N, Rosenberg JN, Oyler GA, et al. Bioprospecting of microalgae for integrated biomass production and phytoremediation of unsterilized wastewater and anaerobic digestion centrate. Appl Microbiol Biotechnol. 2015;99(14):6139–54.
28. Arriola MB, Velmurugan N, Zhang Y, Plunkett MH, Hondzo H, Barney BM. Genome sequences of *Chlorella sorokiniana* UTEX 1602 and *Micractinium conductrix* SAG 241.80: implications to maltose excretion by a green alga. Plant J. 2018;93(3):566–86.
29. Matsuo T, Otsubo Y, Urano J, Tamanoi F, Yamamoto M. Loss of the TOR kinase Tor2 mimics nitrogen starvation and activates the sexual development pathway in fission yeast. Mol Cell Biol. 2007;27(8):3154–64.
30. Liu Y, Duan X, Zhao X, Ding W, Wang Y, Xiong Y. Diverse nitrogen signals activate convergent ROP2-TOR signaling in Arabidopsis. Dev Cell. 2021;56(9):1283-1295.e5.
31. Porstmann T, Santos CR, Griffiths B, Cully M, Wu M, Leevers S, et al. SREBP activity is regulated by mTORC1 and contributes to Akt-dependent cell growth. Cell Metab. 2008;8(3):224–36.
32. Madeira JB, Masuda CA, Maya-Monteiro CM, Matos GS, Montero-Lomelí M, Bozaquel-Morais BL. TORC1 inhibition induces lipid droplet replenishment in yeast. Mol Cell Biol. 2015;35(4):737–46.
33. Li L, Zhu T, Huang L, Ren M. Target of rapamycin signaling involved in the regulation of photosynthesis and cellular metabolism in *Chlorella sorokiniana*. IJMS. 2022;23(13):7451.
34. Thoreen CC, Kang SA, Chang JW, Liu Q, Zhang J, Gao Y, et al. An ATP-competitive mammalian target of rapamycin inhibitor reveals rapamycin-resistant functions of mTORC1. J Biol Chem. 2009;284(12):8023–32.
35. Van Leene J, Han C, Gadeyne A, Eeckhout D, Matthijs C, Cannoot B, et al. Capturing the phosphorylation and protein interaction landscape of the plant TOR kinase. Nat Plants. 2019;5(3):316–27.
36. Schmollinger S, Mühlhaus T, Boyle NR, Blaby IK, Casero D, Mettler T, et al. Nitrogen-sparing mechanisms in Chlamydomonas affect the transcriptome, the proteome, and photosynthetic metabolism. Plant Cell. 2014;26(4):1410–35.
37. Kleessen S, Irgang S, Klie S, Giavalisco P, Nikoloski Z. Integration of transcriptomics and metabolomics data specifies the metabolic response of Chlamydomonas to rapamycin treatment. Plant J. 2015;81(5):822–35.

38. Shpilka T, Welter E, Borovsky N, Amar N, Shimron F, Peleg Y, et al. Fatty acid synthase is preferentially degraded by autophagy upon nitrogen starvation in yeast. Proc Natl Acad Sci USA. 2015;112(5):1434–9.
39. Shi L, Wu Y, Sheen J. TOR signaling in plants: conservation and innovation. Development. 2018;145(13):dev160887.
40. Mubeen U, Jüppner J, Alpers J, Hincha DK, Giavalisco P. Target of rapamycin inhibition in *Chlamydomonas reinhardtii* triggers de Novo amino acid synthesis by enhancing nitrogen assimilation. Plant Cell. 2018;30(10):22401–54.
41. Roustan V, Bakhtiari S, Roustan PJ, Weckwerth W. Quantitative in vivo phosphoproteomics reveals reversible signaling processes during nitrogen starvation and recovery in the biofuel model organism Chlamydomonas reinhardtii. Biotechnol Biofuels. 2017;10(1):1–24.
42. Xiong Y, Sheen J. The role of target of rapamycin signaling networks in plant growth and metabolism. Plant Physiol. 2014;164(2):499–512.
43. Laplante M, Sabatini DM. An emerging role of mTOR in lipid biosynthesis. Curr Biol. 2009;19(22):R1046–52.
44. Caldana C, Li Y, Leisse A, Zhang Y, Bartholomaeus L, Fernie AR, et al. Systemic analysis of inducible target of rapamycin mutants reveal a general metabolic switch controlling growth in *Arabidopsis thaliana*. Plant J. 2013;73(6):897–909.
45. O'Leary BM, Oh GGK, Lee CP, Millar AH. Metabolite regulatory interactions control plant respiratory metabolism via Target of Rapamycin (TOR) kinase activation. Plant Cell. 2020;32(3):666–82.
46. Ingargiola C, Jéhanno I, Forzani C, Marmagne A, Broutin J, Clément G, et al. The Arabidopsis Target of Rapamycin (TOR) kinase regulates ammonium assimilation and glutamine metabolism. Plant Biol. 2022. Cited 2023 Jan 18. Available from: http://biorxiv.org/lookup/doi/10.1101/2022.12.09.519783.
47. Mallén-Ponce MJ, Pérez-Pérez ME, Crespo JL. Deciphering the function and evolution of the target of rapamycin signaling pathway in microalgae. J Exp Bot. 2022;73(20):6993–7005.
48. Sharma M, Sharma M, Jamsheer KM, Laxmi A. A glucose–target of rapamycin signaling axis integrates environmental history of heat stress through maintenance of transcription-associated epigenetic memory in Arabidopsis. Gibbs D, editor. J Exp Bot. 2022;73(20):7083–102.
49. Gorman DS, Levine RP. Cytochrome f and plastocyanin: their sequence in the photosynthetic electron transport chain of *Chlamydomonas reinhardtii*. Proc Natl Acad Sci USA. 1965;54(6):1665–9.
50. Bligh EG, Dyer WJ. A rapid method of total lipid extraction and purification. Can J Biochem Physiol. 1959;37(8):911–7.
51. Pflaster EL, Schwabe MJ, Becker J, Wilkinson MS, Parmer A, Clemente TE, et al. A high-throughput fatty acid profiling screen reveals novel variations in fatty acid biosynthesis in *Chlamydomonas reinhardtii* and related algae. Eukaryot Cell. 2014;13(11):1431–8.
52. Grigoriev IV, Hayes RD, Calhoun S, Kamel B, Wang A, Ahrendt S, et al. PhycoCosm, a comparative algal genomics resource. Nucleic Acids Res. 2021;49(D1):D1004–11.
53. Madeira F, Pearce M, Tivey ARN, Basutkar P, Lee J, Edbali O, et al. Search and sequence analysis tools services from EMBL-EBI in 2022. Nucleic Acids Res. 2022;50(W1):W276–9.
54. Perez-Riverol Y, Bai J, Bandla C, García-Seisdedos D, Hewapathirana S, Kamatchinathan S, et al. The PRIDE database resources in 2022: a hub for mass spectrometry-based proteomics evidences. Nucleic Acids Res. 2022;50(D1):D543–52.

Publisher's Note